frontiers | Frontiers in Nanotechnology

ORIGINAL RESEARCH
published: 20 July 2022
doi: 10.3389/fnano.2022.864644

# Optimizing Colloidal Stability and Transport of Polysaccharide-Coated Magnetic Nanoparticles for Reservoir Management: Effects of Ion Specificity

*Rena Shi, Hooisweng Ow*, Jason R. Cox, Anthony A. Kmetz and Hsieh Chen*

*Aramco Americas Co., Aramco Research Center – Boston, Cambridge, MA, United States*

OPEN ACCESS

***Edited by:***
*Enrico Andreoli,*
*Swansea University, United Kingdom*

***Reviewed by:***
*Soubantika Palchoudhury,*
*University of Dayton, United States*
*Tanapon Phenrat,*
*Naresuan University, Thailand*

****Correspondence:***
*Hooisweng Ow*
*hooisweng.ow@*
*aramcoamericas.com*

***Specialty section:***
*This article was submitted to Nanotechnology for Energy Applications, a section of the journal Frontiers in Nanotechnology*

***Received:*** *28 January 2022*
***Accepted:*** *16 June 2022*
***Published:*** *20 July 2022*

***Citation:***
*Shi R, Ow H, Cox JR, Kmetz AA and Chen H (2022) Optimizing Colloidal Stability and Transport of Polysaccharide-Coated Magnetic Nanoparticles for Reservoir Management: Effects of Ion Specificity. Front. Nanotechnol. 4:864644. doi: 10.3389/fnano.2022.864644*

In this work we explore the mechanisms of ion-specific stabilization of a polysaccharide-based coating for colloidal nanomaterials used within the oil & gas industry. While nanotechnology has wide prevalence across multiple industries, its utility within this sector is largely undeveloped but has potential applications in areas including (but not limited to) exploration, drilling and production processes. For example, reservoir contrast agents in the form of superparamagnetic nanoparticles could be used to accurately determine the residual oil saturation distribution in a reservoir and thus advise enhanced oil recovery (EOR) efforts. However, deployment of such materials in oil reservoirs proves challenging in cases where high salinity subsurface environments induce nanoparticle aggregation, leading to loss of mobility. Here, we report the synthesis and characterization of dextran-coated superparamagnetic iron oxide nanoparticles (Dex-SPIONs), the colloidal stability of which was evaluated in various brine formulations at elevated temperatures. Initial dynamic light scattering (DLS) measurements reveal a lack of contingency between particle stability and total electrolyte concentration for samples comprised of synthetic seawater and low-salinity brine, the latter fluid of which possesses higher ionic strength yet preserves colloidal integrity to a much greater extent than its seawater counterpart. Further experiments point to a calcium ($Ca^{2+}$) ion-specific stabilization effect wherein surface complexation of $Ca^{2+}$ ions to the dextran periphery improves carbohydrate hydration and thus enhances colloidal stability. Ion selective electrode (ISE) measurements provide additional evidence of the $Ca^{2+}$ - dextran binding interaction, the role of which also factors significantly into mitigation of polysaccharide degradation [as demonstrated through gel permeation chromatography (GPC)]. Finally, we assess the transport of Dex-SPIONs through porous media, including examination of retention properties with respect to variances in ionic composition.

**Keywords: specific ion effects, superparamagnetic iron oxide nanoparticles, colloidal stability, polysaccharide coatings, downhole applications**

## 1 INTRODUCTION

Understanding the fate and transport of nanomaterials in subsurface environments has far reaching implications in fields ranging from enhanced oil recovery (EOR) to environmental remediation. (Amanullah and Al-Tahini 2009; Halford 2012; Hashemi et al., 2014; Hotze et al., 2010; Ju and Fan 2009; McElfresh et al., 2012; Nabhani et al.,; Yu et al., 2012; Yu et al., 2010; T. Zhang et al., 2015). As such, much attention has been directed towards developing coating chemistries that are capable of stabilizing nanomaterials in harsh subterranean environments (ShamsiJazeyi et al., 2014; Xue et al., 2014). Intricate strategies have been developed to facilitate the use of nanomaterials in such conditions, mainly focusing on coating chemistries that leverage electrostatic, steric and/or electrosteric repulsion to prevent colloid aggregation (Ponnapati et al., 2011; McElfresh et al., 2012; Bagaria et al., 2013; ShamsiJazeyi et al., 2014; Xue et al., 2014). Despite this success, the particularly challenging conditions encountered in oil reservoirs, where the downhole temperature frequently exceeds 100°C and the salinity reaches levels of 220,000 ppm total dissolved solids (TDS), (Lynn and Nasr-El-Din 1998), have proven difficult to surmount. These difficulties arise due to charge screening by electrolytes in the concentrated brine and by high temperatures which often lead to collapse of the steric layer due to lower critical solution temperature (LCST) transitions of the coating layer (Principles of Colloid and Surface Chemistry 1997; Matteucci et al., 2008; Kotsmar et al., 2010). The latter point is exemplified by the failure of polyethylene glycol coatings to stabilize colloids at elevated temperatures in saline solution, whereas the room temperature performance of the same coating in saline solution is quite satisfactory (Worthen et al., 2016).

Within the broad scope of engineered nanomaterials, a considerable amount of interest has been placed in the application of iron-based nanoparticles, specifically superparamagnetic iron oxide nanoparticles (SPIONs) and nanoscale zero-valent iron (nZVI), as contrast agents for magnetic resonance imaging and for environmental remediation, respectively. Dextran-coated superparamagnetic iron oxide nanoparticles (Dex-SPIONs) have shown promise in clinical applications as magnetic resonance imaging (MRI) contrast agents, providing enhanced image quality at lower particle concentrations relative to their nearest polymer-coated counterparts (Unterweger et al., 2018; Nelson et al., 2020). Surface-reactive nanoscale zero-valent iron nanoparticles have been explored as *in situ* reducing agents for the de-chlorination of chlorinated solvent contaminants present in soil and groundwater, and as adsorbents of heavy metals (Zhao et al., 2016). However, due to their high surface energy and magnetic attraction bare nZVI nanoparticles are extremely prone to aggregation, not to mention loss of reactivity through interactions with surrounding media (Mondal, Jegadeesan, and Lalvani 2004; Zhao et al., 2016). To mitigate aggregation and low transportability, methods for surface modification of nZVI have been explored via polymeric coatings, e.g. biopolymers. Humic acid and calcium ions present in groundwater are postulated to have an effect on surface-modified nanoparticle stability through destabilizing bridging interactions that are highly dependent on groundwater geochemistry (Dong and Lo 2013), making it difficult to predict nZVI transport in the subsurface. Dong et al. reported that different surface-modified nZVIs led to varying stability characteristics; yet, regardless of the stabilization mechanism (polyelectrolyte, non-ionic surfactant, potato starch) the results remained largely the same in that aggregation and sedimentation could not be mitigated under the examined circumstances (Dong and Lo 2013).

In an effort to advance the development of technologies that would enable the use of nanomaterials in oilfield exploration, we embarked on a program to identify coating systems capable of withstanding high salinities through leveraging synergistic interactions between functional groups present on the periphery of nanoparticles and ions present in the brine. This type of interaction, known as an ion specific effect, has received considerable attention within the scientific community (Boström et al., 2001; Deniz et al., 2008; Kunz 2010; X.; Li and Shantz 2010; Pfeiffer et al., 2014; Vereda et al., 2015; Y.; Zhang and Cremer 2006). Intense research aimed at developing a mechanistic understanding of how specific ions interact with macromolecules, interfaces and colloids paints a picture much different than one would intuitively expect, namely that ions can behave in disparate ways despite possessing the same charge valency. This phenomenon is illustrated by cases where colloids and nanoparticles have been re-stabilized in concentrated electrolyte medium through addition of excess electrolyte after having passed through a region of instability at lower ionic strength; the minimum electrolyte concentration at which the colloid becomes stable against aggregation is known as the critical stabilization concentration (CSC) (Healy et al., 1978; Molina-Bolívar et al., 1997; Molina-Bolıvar et al., 1998; Molina-Bolivar et al., 1999; López-León et al., 2005; Santander-Ortega et al., 2010; Santander-Ortega et al., 2011). The majority of this work has focused on examining how a single ion (or electrolyte pair) can influence the behavior of processes ranging from colloidal stability to changes in interfacial tension. Surprisingly, much less emphasis has been placed on examining the role of specific ion effects in multicomponent complex brines.

Thus, the work presented here aims to provide insight into the synergistic interactions occurring between certain divalent ions and carbohydrate-based coatings, namely dextran, to yield colloids with exceptional stability in high ionic strength multicomponent brines. To this end, we have synthesized Dex-SPIONs and tested their colloidal stability in various brine formulations as well as their transport properties in Ottawa sand. Utilization of sand as a medium for characterizing mobility enables benchmarking against transport studies of state-of-the-art engineered nanoparticles also tailored for reservoir applications (Xue et al., 2014). We observe that the presence of calcium ions appears to boost the colloidal stability of polysaccharide-coated nanoparticles in concentrated brines, a possible paradigm shift in designing coatings for subsurface applications. Separately, from a transport perspective, when decoupled from colloidal stability we find that the total ionic strength of the fluid rather than a specific ion effect dominates the retention behavior of the particles in column experiments.

# 2 EXPERIMENTAL

## 2.1 Materials

Dextran-low fraction for biochemistry ($M_w$~90 kDa), iron(III) chloride hexahydrate, iron(II) chloride tetrahydrate, sodium borohydride, sodium hydroxide, 30% ammonium hydroxide, tris buffer (2 M), magnesium chloride hexahydrate and calcium chloride dihydrate were obtained from Fisher Scientific (Fair Lawn, NJ) and used as received. Pentaerythritol glycidyl ether was obtained from Frontier Scientific, Inc. (Logan, UT) and used as received. Water was double-deionized using a Millipore Milli-Q system to produce 18 MΩ deionized water. Sealable 5 ml borosilicate microwave vials were obtained from Chemglass, Inc. (Vineland, NJ) and used as received. Tangential flow filtration for purification of synthesized Dex-SPIONS was performed using a KrosFlo Research Iii TFF system from Spectrum Labs, Inc. (Rancho Dominguez, CA). Preparation of stock electrolyte and brine compositions used in evaluation of colloidal stability is detailed in the supporting information.

### 2.1.1 Synthesis of Dextran-Coated Superparamagnetic Iron Oxide Nanoparticles

Dex-SPIONs were prepared using a procedure reported by Weissleder et al. (Tassa et al., 2011) with slight modification. A round-bottomed flask (200 ml) was charged with a stir bar, 50 ml of deionized water and $FeCl_3$ $6H_2O$ (1.35 g, 0.005 mol). Dextran (3.0 g, 90 kDa $M_w$) was then added, followed by cooling of the reaction vessel to 5°C through the use of an ice water bath and subsequent deoxygenation via nitrogen bubbling. This deoxygenation/cooling cycle was applied for 30 min with vigorous stirring. After 30 min, $FeCl_2$ $4H_2O$ (0.54 g, 0.0027 mol) was dissolved in 5 ml of deionized water and added to the vessel, after which the mixture was allowed to stir under an $N_2$ atmosphere for an additional 10 min. Then, $NH_4OH$ solution (3 ml, 30% w/w) was added dropwise to the mixture over a period of 15 min; as the addition proceeded, the reaction color changed from orange to dark brown/black. The reaction was subsequently heated to 80°C for 45 min, then allowed to cool to room temperature. At this stage, the resulting particles possess a non-covalent dextran coating but require crosslinking to ensure that the coating will remain intact during subterranean operations. In a separate crosslinking procedure, pentaerythritol glycidyl ether (2 ml) was added to 1 M aqueous NaOH (200 ml) and $NaBH_4$ (400 mg) in a round bottom flask (500 ml). A 100 ml addition funnel was mounted to the round bottom flask containing the crosslinking formulation and subsequently charged with the crude nanoparticle dispersion (58 ml), which was added dropwise over a period of approximately 1 h to the crosslinking solution, with vigorous stirring. Following the addition, the reaction was allowed to proceed at room temperature for 24 h. Upon reaction completion, 2M 2-amino-2-hydroxymethyl-propane-1,3-diol (20 ml) was added to the crude mixture to quench unreacted crosslinker; the reaction was allowed to proceed at room temperature for 12 h. The resulting mixture was purified *via* tangential flow filtration (100K MWCO filter) to provide a nanoparticle dispersion with a nominal Dex-SPION concentration of 2,250* ppm (280 ml). *Based on iron oxide content, as determined by thermogravimetric analysis.

### 2.1.2 Cryo-Transmission Electron Microscopy

Dex-SPION at 200 ppm concentration in various brines solutions were imaged without dilution. C-flat copper grids with 1.2 μm holes on the 5 nm carbon support film were used as substrates. 5 μL of the diluted samples were drop-casted on the grid and blotted for 2 s before freezing. Plunge freezing was performed on a Gatan CP3 Cryoplunge at the Harvard University's Center of Nanoscale Systems (CNS) using liquid ethane as cryogen. Samples were loaded onto an FEI Tecnai Arctica CryoTEM at the Harvard CNS and imaged at 200 kV accelerating voltage.

### 2.1.3 Colloidal Stability Testing Protocol

#### *2.1.3.1 Stability in the Presence of Divalent Ions*

The potential impact of calcium and magnesium ions on the colloidal stability of Dex-SPIONS was primarily investigated via a series of heating experiments. Brines composed of 0.5 M $MgCl_2$ doped with varying amounts of $CaCl_2$ were used to generate the following series of stock solutions: 0.5 M $MgCl_2$, 0.5 M $MgCl_2$/0.05 M $CaCl_2$, 0.5 M $MgCl_2$/0.1 M $CaCl_2$, 0.5 M $MgCl_2$/0.2 M $CaCl_2$, and 0.5 M $MgCl_2$/0.5 M $CaCl_2$. A 500 μL aliquot of Dex-SPION stock was added to each 3.5 ml of each respective electrolyte solution to achieve concentrations of 500 ppm across all samples. Neutralized and deoxygenated ($N_2$ purged) samples were subsequently subjected to heating at 103°C over a period of 4–5 days, with particle stability monitored through DLS and visual observation. To further probe the effects of calcium as a specific ion on colloidal stability, Dex-SPIONS were also dispersed in tap water, deionized water, 0.5 mM $CaCl_2$, 5 mM $CaCl_2$, and 50 mM $CaCl_2$, the only variations from dual $Ca^{2+}$/$Mg^{2+}$ studies being in electrolyte concentration and duration of measurement. Operational details regarding DLS measurements are provided in the supporting information.

#### *2.1.3.2 Stability in Representative Reservoir Fluids*

Stock solution of Dex-SPION dispersion (in DI water) was diluted into either seawater or low-salinity brine to yield 200 ppm Dex-SPION nanoparticle dispersions. The sols were pipetted inside 5 ml microwave vials which were subsequently crimp-sealed with PTFE lined aluminum septa. Three replicates of each nanoparticle dispersion were placed in a thermostat regulated oven operating at 103°C. An additional set of duplicates of each nanoparticle dispersion was kept at room temperature to serve as control samples.

# 3 RESULTS

## 3.1 Dextran-Coated Superparamagnetic Iron Oxide Nanoparticles Synthesis and Characterization

Dex-SPIONs were synthesized according to the cold gelation approach as previously referenced. Crosslinking of dextran around the periphery of the nanoparticle was carried out using

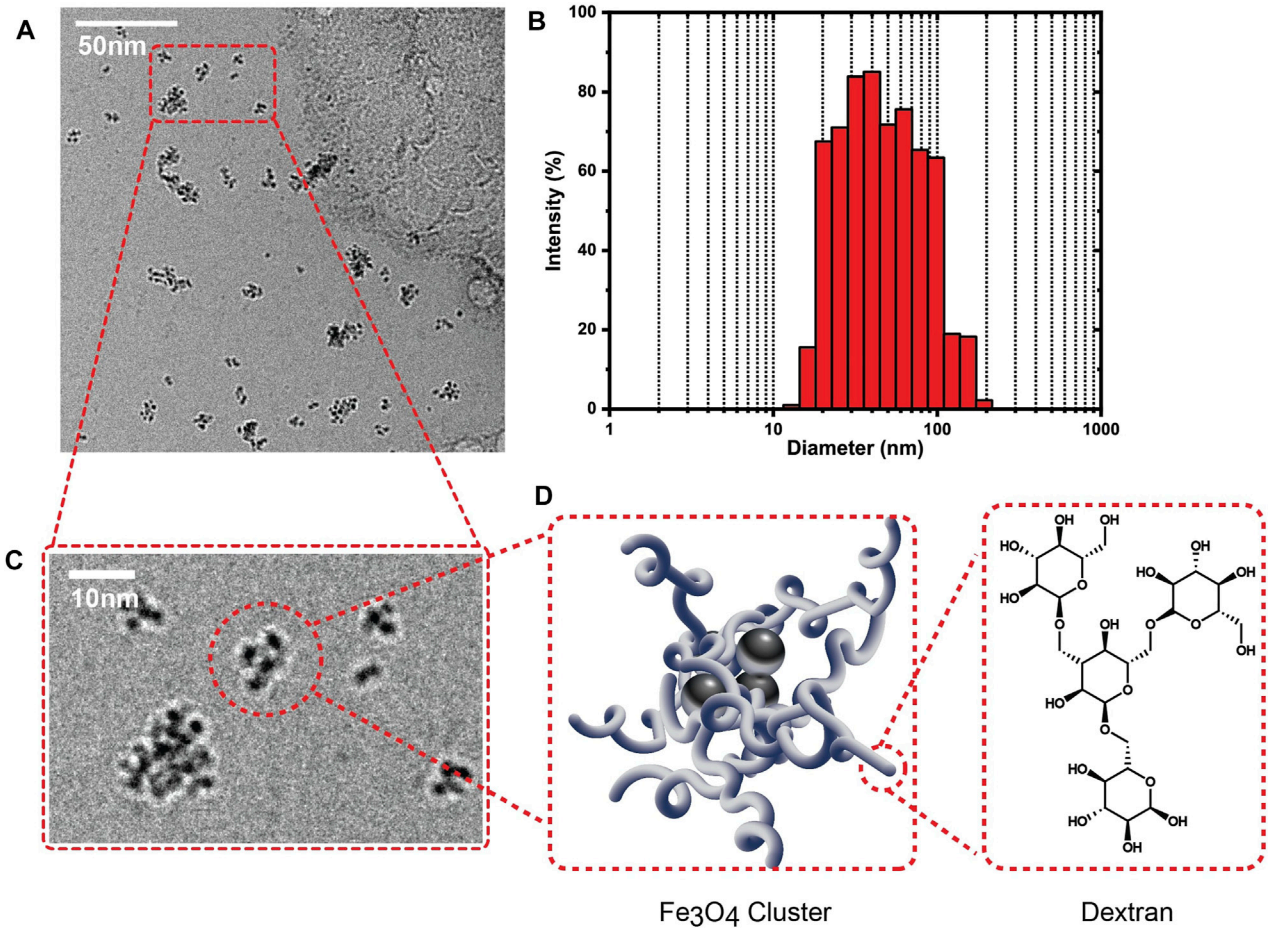


**FIGURE 1 | (A)** Cryo-TEM image of Dex-SPIONs in DI water. **(B)** Graph showing (intensity) average size distribution of Dex-SPIONs. **(C)** Magnified cryo-TEM image of Dex-SPIONs. **(D)** Schematic depicting arrangement of dextran on periphery of a SPION bundle, featuring an inset of the atomistic structure of a dextran fragment.

the tetra-crosslinker pentaerythritol glycidyl ether. Purification of the resulting nanoparticles via tangential flow filtration afforded superparamagnetic nanoparticles with an intensity average hydrodynamic diameter centered around 50 nm (**Figure 1B**). Examination of the nanoparticles using cryo-TEM (**Figures 1A,C**) reveals that the nanoparticles are actually clusters of magnetite crystallites that average 7 nm in diameter. These clusters are presumably held together by the crosslinked dextran shell which also increases the hydrodynamic diameter of the assembly due to its extended conformation in aqueous media.

## 3.2 Dextran-Coated Superparamagnetic Iron Oxide Nanoparticles Colloidal Stability in Representative Reservoir Fluids

As ultimate reservoir deployment of Dex-SPIONs is contingent upon their compatibility with reservoir fluids, evaluation of their stability in representative multi-valent/component brines proves crucial. The colloidal stability of Dex-SPIONs was followed via DLS at 103°C in both seawater and brine over the course of 2 weeks. As shown in **Figure 2A**, the colloidal stability of Dex-SPIONs in brine is satisfactory, however; the case in seawater is different as the average hydrodynamic diameter of the nanoparticles increases as a function of time—an early indication of colloidal instability. Initially, we were surprised by this result as the total electrolyte content of seawater is substantially less than that of brine. To investigate further, we proceeded to conduct a root cause analysis to identify if a particular ion present in the seawater was responsible for the decreased stability. The results of this study are depicted in **Figure 2B** which displays the hydrodynamic diameter of the nanoparticles as a function of time at 103°C in various salt solutions. Each salt component is present within the seawater formulation and is of the concentration as it exists in seawater. As can be seen from the results, magnesium is the only ion that leads to an increase in hydrodynamic diameter as a function of incubation time. Similar to earlier observations, an initial salt- and/or heating-induced dehydration event occurs across all samples in the initial 2-day time period before individual salt influences take full effect.

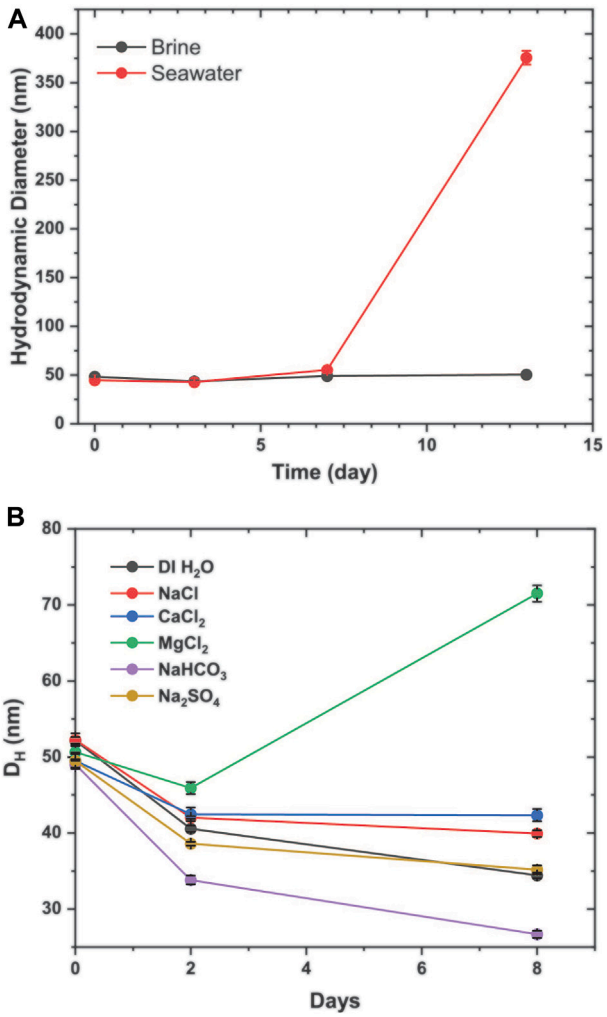


**FIGURE 2 | (A)** DLS graphs of the average hydrodynamic diameter of Dex-SPIONS in seawater (left) and brine (right) versus elapsed time at 103°C. **(B)** Average hydrodynamic diameters of dextran-coated nanoparticles as a function of heating at 103°C in various electrolyte solutions for the specified time intervals. NaCl = 700 mM; $CaCl_2$ = 16 mM; $MgCl_2$ = 87 mM; $NaHCO_3$ = 2 mM; $Na_2SO_4$ = 45 mM.

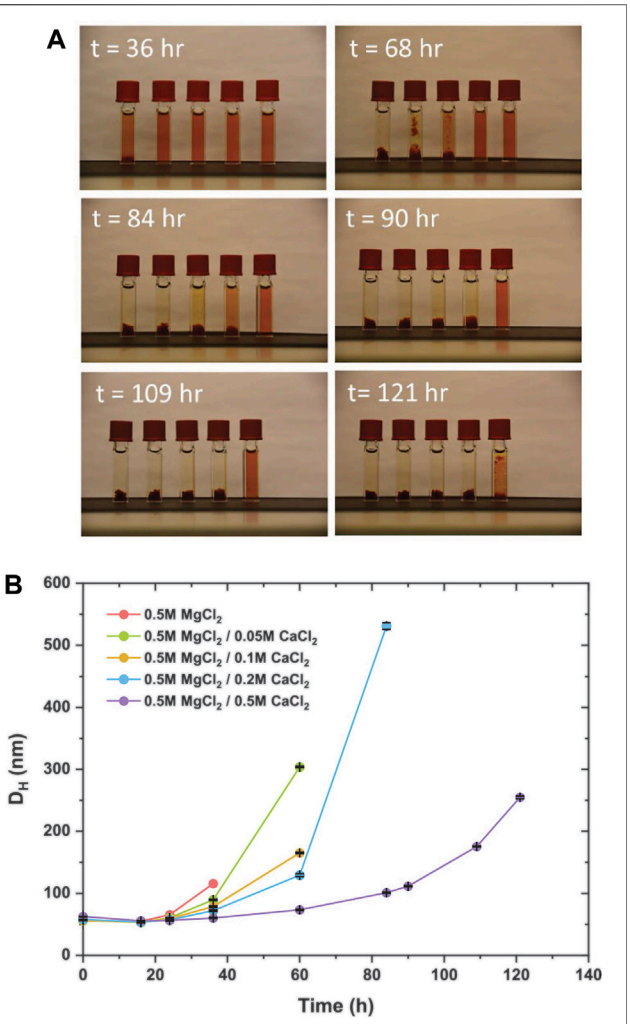


**FIGURE 3 | (A)** Time-lapse images of Dex-SPIONS dispersed in the following brine compositions (left-to-right, per time point): 0.5 M $MgCl_2$, 0.5 M $MgCl_2$/0.05 M $CaCl_2$, 0.5 M $MgCl_2$/0.1 M $CaCl_2$, 0.5 M $MgCl_2$/0.2 M $CaCl_2$, and 0.5 M $MgCl_2$/0.5 M $CaCl_2$. **(B)** DLS graph showing average hydrodynamic diameter as a function of time spent under heating at 103°C.

This preliminary result was indeed surprising as magnesium is also present in brine (see **Supplementary Table S1**) yet the nanoparticles are quite stable in this media; however, brine also possesses a much higher concentration of $CaCl_2$ in comparison with seawater, suggesting that $Ca^{2+}$ may serve as the mitigating ion present in brine that off-sets the instabilities caused by magnesium salts, thus stabilizing the Dex-SPIONs against their coating-dependent aggregation.

## 3.3 Dextran-Coated Superparamagnetic Iron Oxide Nanoparticles Colloidal Stability in the Presence of Divalent Ions

Divalent ions such as calcium and magnesium pose the greatest challenge to the colloidal stability of nanomaterials in natural fluids such as connate and seawater. Within subsurface environments, high salinities bear strong association with nanoparticle aggregation, thus hindering their mobility (Y. Li et al., 2008; Saleh et al., 2008). With the predominance of $Ca^{2+}$ and $Mg^{2+}$ ions in synthetic seawater and low-salinity brine, an investigation into their potential (de)stabilizing effects is necessary. Dex-SPIONs were dispersed into aqueous media containing varying concentrations of $CaCl_2$ and $MgCl_2$, and the resulting solutions were subjected to continuous heating. Initial evidence of sample precipitation occurs after 36 h of heating (**Figure 3A**, t = 36 h), at which point the left-most sample containing solely magnesium salts begins to precipitate. Our following observations suggest a definite correlation between colloidal stability and the amount of calcium present in solution, as prolonged heating induces sample precipitation

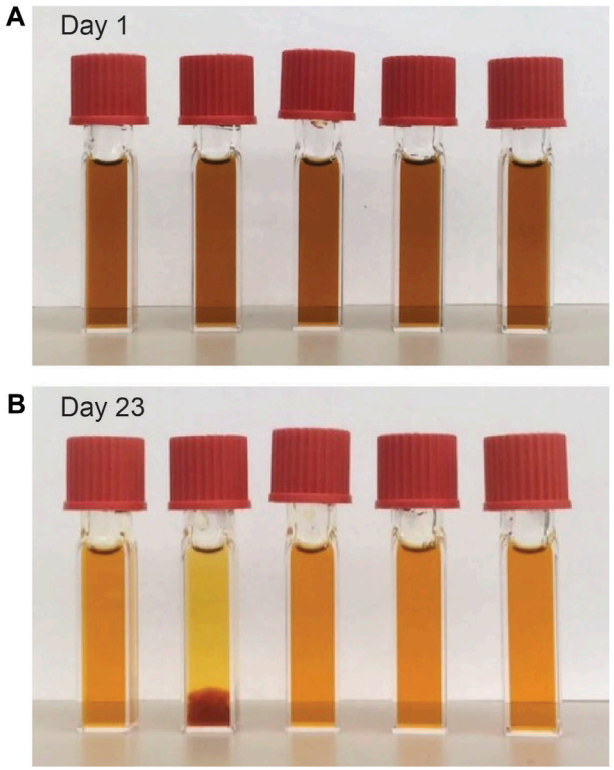


**FIGURE 4 | (A)** Dex-SPIONS dispersed in (left-to-right) tap, deionized water, 0.5 mM $CaCl_2$, 1 mM $CaCl_2$, and 50 mM $CaCl_2$ at room temperature. **(B)** The same series after 23 days of heating at 103°C.

occurring in a seemingly ordered manner consistent with the hypothesis that brines containing higher levels of $Ca^{2+}$ enable preservation of colloidal integrity for longer periods of time; with increasing $Ca^{2+}$ concentration comes greater delays in particle growth/aggregation, as monitored by DLS (**Figure 3B**). As the DLS instrument measures each sample in triplicate, average particle sizes were calculated and plotted, with the standard deviation(s) included as y-error. Notably, within the first 24 h (approx.) all 5 samples experience an initial reduction/stagnation in particle growth which may be attributed to a temporary dehydration effect that occurs in the early stages of heating, leading to reductions in measured hydrodynamic diameters of Dex-SPIONs.

**Figure 4** summarizes the results of further investigations into the singular, possibly stabilizing role of $Ca^{2+}$ ions. Tap and deionized water were included within the series of electrolyte solutions as references. All Dex-SPION-containing dispersions were found to be stable at room temperature (**Figure 4A**), both initially and over time; however, precipitation of the deionized water sample occurred after 23 days of heating at 103°C (**Figure 4B**). Under the premise that calcium ions provide stabilizing effects, the lack of calcium in deionized water implies that no ion-specific stabilization is afforded; survivability of the tap water sample, however, may be attributed to the intrinsic calcium content of tap water (Morr et al., 2006).

## 3.4 Ion Selective Electrode Measurements

Real-time analysis of calcium-dextran binding activity was performed using a $Ca^{2+}$- selective electrode, wherein dextran solution was gradually titrated into electrolyte solution under stirring and the changes in $[Ca^{2+}]$ measured. Experimental details regarding electrode usage are outlined in the supporting information. Prior to the addition of dextran solution, the initial measured ionic activity of $Ca^{2+}$ was 10.8 mM (**Figure 5**); if we solely account for the effects of dilution, the resulting $Ca^{2+}$ activity upon completion of dextran addition should be equal to 10.3 mM. The discrepancy between this value and the measured value of 9.7 mM, however, indicates the possibility of $Ca^{2+}$ binding to the dextran periphery that would then lead to a decrease in the presence of free calcium ions able to be detected.

## 3.5 Oxidative Degradation of Dextran as Studied by Gel Permeation Chromatography

To better understand the extent of coating stabilization of our Dex-SPION nanoparticles, we chose to examine the degradation mechanics of dextran alone under exposure to reservoir conditions, both at atmosphere (in the presence of oxygen) and under deoxygenated conditions ($N_2$ purged). Aqueous gel permeation chromatography (GPC) provides a means to detect changes in molecular weight distributions of dextran and its degradative products based on size-exclusion principles. Our results show that the molecular weight distribution of dextran dissolved in both DI water and seawater (abbreviated as DI and SW, respectively) does not change (after 7 days) with respect to their respective room temperature controls, implying that degradation does not occur even at elevated temperatures and in the presence of oxygen (**Figures 6A,B**). Conversely, GPC analysis of dextran dissolved in both brine and tap water (abbreviated as LSB and Tap, respectively) shows changes in elution volume and detector response that are indicative of

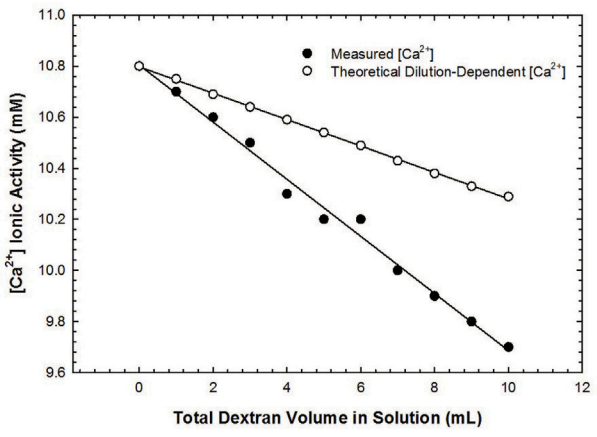


**FIGURE 5 |** Change in calcium ion concentration as a function of dextran added.

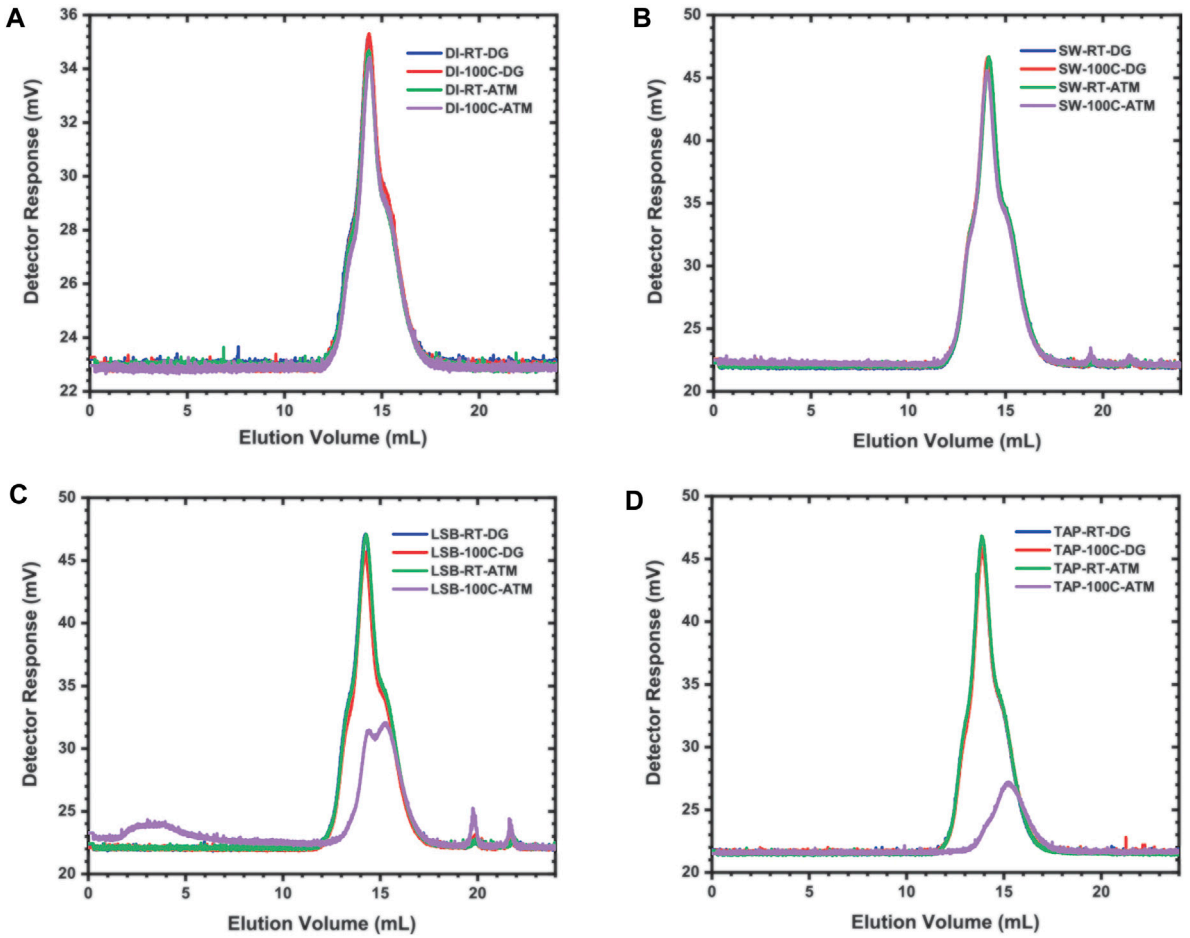


**FIGURE 6 |** GPC chromatograms depicting elution of dextran dissolved in deionized water (DI), seawater (SW), low-salinity brine (LSB) and tap water (TAP), including elution of its molecular weight fragments. RT = room temperature, 100C = heated sample, DG = degassed (purged with $N_2$), ATM = sealed under regular atmosphere.

molecular weight fragmentation, in reference to the lowest elution curve in each plot that represents samples sealed under regular atmosphere and subjected to heating, labeled as LSB-100C-ATM and Tap-100C-ATM (**Figures 6C,D**). To explain this phenomenon, we postulate that elevated levels of $Ca^{2+}$ present in brine in comparison with seawater lead to maximized ion-polysaccharide interactions, allowing the dextran polymer to maintain an extended conformation. In this state, the polymer is more prone to degradation via chain scission catalyzed by the presence of heat and oxygen, causing changes in its molecular weight distribution and resulting in the differing GPC elution/detector response; presumably, the presence of calcium in tap water also gives rise to similar results (Xue et al., 2014). Although calcium is present in seawater, the concentration is much less than in brine and as such, the relative abundance of magnesium salts may exert opposing effects, as suggested by previous work (Morr et al., 2006). The implications of this include poorer solvation of dextran that causes the polymer to remain in a shrunken conformation. In this condensed form, the probability of chain scission is minimized as the polymer backbone is shielded from its surrounding environment. In DI water, dextran maintains this same conformation, thus accounting for the lack of degradation observed.

## 3.6 Sand Pack Transport Experiments

The purpose of the sand pack column transport experiments is twofold—1) to assess the mobility and stability of the Dex-SPIONS as they traverse a porous medium; and 2) to study the effect of ionic composition on the irreversible retention and arrival time of the Dex-SPIONs. Firstly, the assessment of mobility is important with respect to the robustness of the dextran coating. The bulk of prior experiments herein are performed in batch settings and the Dex-SPIONs are not subjected to any shearing effects that may compromise the coating. Although Ottawa sand is a relatively homogenous porous medium compared to consolidated rocks in nature, the tortuosity of the flow paths is significant enough to be deemed suitable for evaluating the fate and transport of engineered nanomaterials (Morr et al., 2006; Saleh et al., 2008; Xue et al., 2014). Each experimental injection contains a Dex-SPION

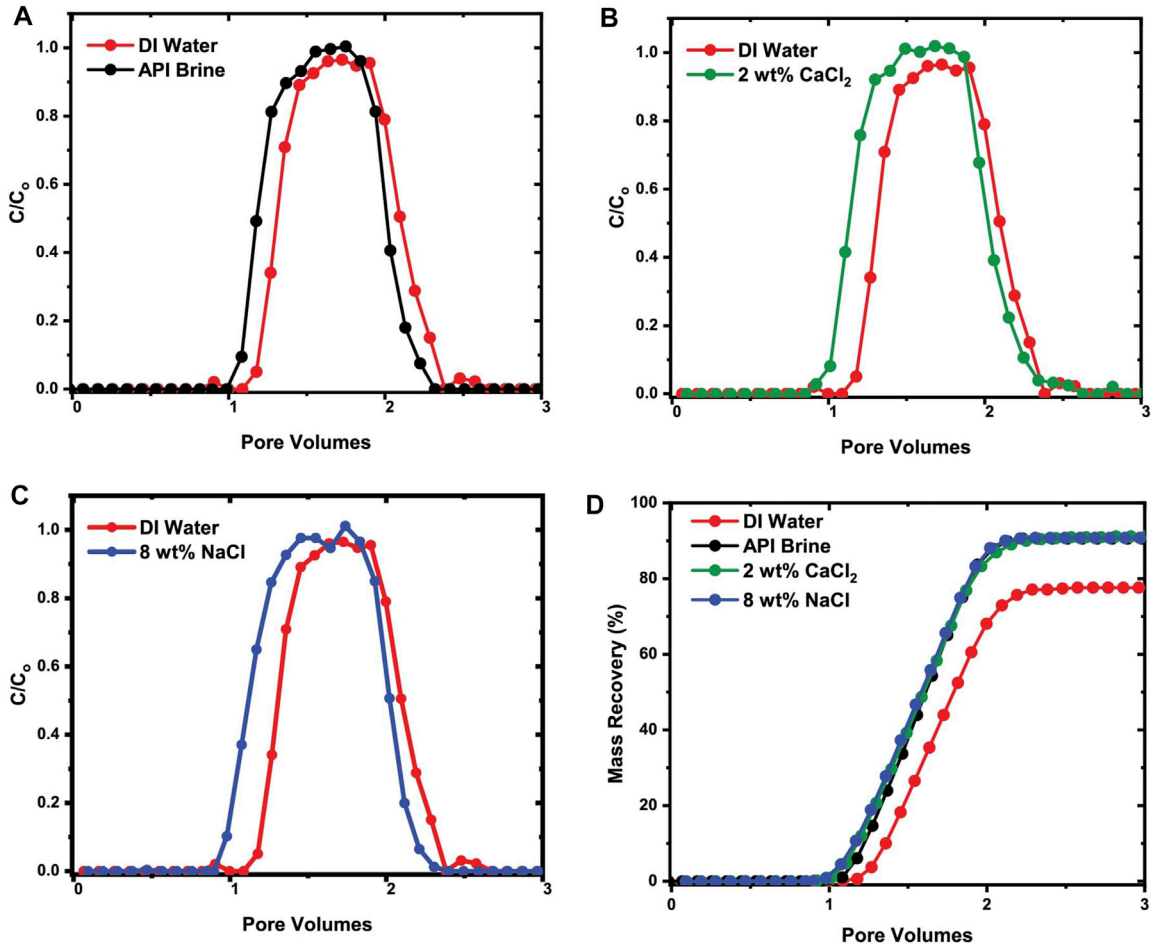


**FIGURE 7 |** Effluent breakthrough curves from column chromatography sand pack experiments showing the difference in the transport and mass recovery between Dex-SPIONs in DI water and in various ionic solutions, i.e. API brine and calcium chloride ($CaCl_2$) / sodium chloride (NaCl) solution.

**TABLE 1 |** Summary of results from sand pack transport experiments.

| Nanoparticle source & type[a] | Porous media[b] | Aqueous phase[c] | $V_{disp}$[d] (ft/day) | NP pulse[e] (PV) | BT[f] (%) | Retention[g] (μg/g) |
|---|---|---|---|---|---|---|
| ASC Dex-SPION | 40–50 mesh unwashed OS | DI Water | 2.5 | 1.0 | 77.8 | 30 |
| ASC Dex-SPION | 40–50 mesh unwashed OS | API Brine | 2.5 | 1.0 | 91.6 | 11 |
| ASC Dex-SPION | 40–50 mesh unwashed OS | 8 wt% NaCl | 2.5 | 1.0 | 90.7 | 13 |
| ASC Dex-SPION | 40–50 mesh unwashed OS | 2 wt% $CaCl_2$ | 2.5 | 1.0 | 91.1 | 13 |
| ASC Dex-SPION | 40–50 mesh unwashed OS | API Brine | 2.5 | 3.0 | 99.2 | 9 |
| UT-Austin nMag[39] | 40–50 mesh unwashed OS | API Brine | 2.5 | 3.0 | 80.1 | 72* |

[a]*ASC Dex-SPION, Aramco Services Company – Dextran coated superparamagnetic iron oxide nanoparticle; UT-Austin nMag, University of Texas at Austin nano-magnetite (iron-oxide) from Kmetz et al., 2016.*

[b]*OS, unwashed Ottawa sand, 99% quartz, 297–420 μm diameter grains.*

[c]*Aqueous phase, salinity of fluid used to saturate the column and inject nanoparticle solution with; API brine, American Petroleum Institute brine comprising of 8 wt% NaCl and 2 wt% $CaCl_2$.*

[d]*$V_{disp}$, average injection velocity of displacement front across column.*

[e]*NP Pulse, Volume of injected nanoparticle solution in pore volumes.*

[f]*BT, percentage of recovered mass over injected mass aka breakthrough percentage.*

[g]*Retention, mass of nanoparticle irreversibly retained per mass of porous media; better known as normalized retention.*

**Modeled max, solid phase retention annotated as $S_{max}$ in publication.*

concentration of 625 ppm in their respective ionic solution and spans a pulse width of 3 pore volumes.

**Figures 7A–C** show the normalized effluent concentration curves of Dex-SPIONS in various ionic solutions compared to those of Dex-SPIONs in DI water. The most telling artifact of these experiments is the slight delay in the arrival of Dex-SPIONs in DI water (shown by the red curves) in comparison with that of Dex-SPIONs in ionic media, as well as the observation that parity with the injected concentration does not quite reach $C/C_0 = 1.0$ (100% of input concentration). Both the delays in arrival and lower peak effluent concentrations are indicative of retention and perhaps irreversible loss due to adsorption. The mass recovery of the Dex-SPIONs as a function of eluted pore volumes is shown in **Figure 7D**.

To quantify Dex-SPION transport as a function of ionic solution, a mass balance of the injected pulse and subsequent flush of Dex-SPION-free ionic solution was kept to track material not collected in effluent samples. Below in **Table 1**, a full summary of the experimental results can be found. Even though the results were considered to be extremely promising, they could not be completely appreciated until an external benchmark could be drawn for comparison. Thus, an experiment in API brine with a Dex-SPION pulse width of 3 PVs was conducted with a setup and conditions equal to that detailed in Kmetz et al., 2016. (Kmetz et al., 2016). In the direct comparison, it is appropriate to compare total SPION recovery given all other parameters were equal. Approximately 99% of Dex-SPIONs were recovered in effluent samples whereas the external study recovered only about 80% of the injected nanoparticles. Likewise, the solid phase irreversible retention was approximately 7x′s larger in the external study.

## 4 CONCLUSION

In summary, the study detailed here describes and characterizes the phenomena dealing with calcium-ion specific binding to polysaccharides, namely dextran. Broader implications include the stabilization of colloids within harsh environments, as highlighted by recent efforts towards exploiting functional nanomaterials for hydrocarbon exploration within subsurface oil reservoirs as well as for production applications (Kanj et al., 2011; Chen et al., 2015; Chen et al., 2016). In addressing this issue, we show that superparamagnetic iron-oxide nanoparticles (SPIONs) coated with dextran exhibit colloidal stability at high temperatures over a period of several days, as enabled by synergistic interactions between $Ca^{2+}$ and the carbohydrate periphery. While there still remain extensive challenges to overcome, we hope that the observations presented here serve as valuable contributions towards the development of robust coating chemistries for materials deployed not only for oil & gas applications but across multiple industries.

## DATA AVAILABILITY STATEMENT

The original contributions presented in the study are included in the article/**Supplementary Material,** further inquiries can be directed to the corresponding author.

## AUTHOR CONTRIBUTIONS

All authors listed have made a substantial, direct, and intellectual contribution to the work and approved it for publication.

## FUNDING

This work was funded by Saudi Aramco and Aramco Services Company. This work was performed in part at the Center for Nanoscale Systems (CNS), a member of the National Nanotechnology Infrastructure Network (NNIN), which is supported by the National Science Foundation under NSF award no. ECS-0335765. CNS is part of Harvard University.

## ACKNOWLEDGMENTS

We thank Aramco Research Center – Boston, Reservoir Engineering Technology team members for valuable discussion and suggestions. We also thank Saudi Aramco and Aramco Services Company for kindly allowing us to publish this work.

## SUPPLEMENTARY MATERIAL

The Supplementary Material for this article can be found online at: https://www.frontiersin.org/articles/10.3389/fnano.2022.864644/full#supplementary-material

## REFERENCES

Amanullah, M., and Al-Tahini, A. M. (2009). "Nano-Technology - its Significance in Smart Fluid Development for Oil and Gas Field Application," in Paper presented at the SPE Saudi Arabia Section Technical Symposium, Al-Khobar, Saudi Arabia, May 2009. doi:10.2118/126102-ms

Bagaria, H. G., Xue, Z., Neilson, B. M., Worthen, A. J., Yoon, K. Y., Nayak, S., et al. (2013). Iron Oxide Nanoparticles Grafted with Sulfonated Copolymers Are Stable in Concentrated Brine at Elevated Temperatures and Weakly Adsorb on Silica. *ACS Appl. Mater. Interfaces* 5 (8), 3329–3339. doi:10.1021/am4003974

Boström, M., Williams, D. R. M., and Ninham, B. W. (2001). Specific Ion Effects: Why DLVO Theory Fails for Biology and Colloid Systems. *Phys. Rev. Lett.* 87 (16), 168103.

Chen, H., Cox, J. R., Ow, H., Shi, R., and Panagiotopoulos, A. Z. (2016). Hydration Repulsion between Carbohydrate Surfaces Mediated by Temperature and Specific Ions. *Sci. Rep.* 6 (1), 28553–28610. doi:10.1038/srep28553

Chen, H., Panagiotopoulos, A. Z., and Giannelis, E. P. (2015). Atomistic Molecular Dynamics Simulations of Carbohydrate-Calcite Interactions in Concentrated Brine. *Langmuir* 31 (8), 2407–2413. doi:10.1021/la504595g

Deniz, V., Boström, M., Bratko, D., Tavares, F. W., and Ninham, B. W. (2008). Specific Ion Effects: Interaction between Nanoparticles in Electrolyte Solutions. *Colloids Surfaces A Physicochem. Eng. Aspects* 319 (1-3), 98–102. doi:10.1016/j.colsurfa.2007.08.020

Dong, H., and Lo, I. M. C. (2013). Influence of Calcium Ions on the Colloidal Stability of Surface-Modified Nano Zero-Valent Iron in the Absence or Presence of Humic Acid. *Water Res.* 47 (7), 2489–2496. doi:10.1016/j.watres.2013.02.022

Halford, B. (2012). Nanotech Strikes Oil. *Chem. Eng. News Arch.* 90, 60–62. doi:10.1021/cen-09011-scitech2

Hashemi, R., Nassar, N. N., and Pereira Almao, P. (2014). Nanoparticle Technology for Heavy Oil *In-Situ* Upgrading and Recovery Enhancement: Opportunities and Challenges. *Appl. Energy* 133, 374–387. doi:10.1016/j.apenergy.2014.07.069

Healy, T. W., Homola, A., James, R. O., and Hunter, R. J. (1978). Coagulation of Amphoteric Latex Colloids: Reversibility and Specific Ion Effects. *Faraday Discuss. Chem. Soc.* 65, 156–163. doi:10.1039/dc9786500156

Hotze, E. M., Phenrat, T., and Lowry, G. V. 2010. "Nanoparticle Aggregation: Challenges to Understanding Transport and Reactivity in the Environment." *J. Environ. Qual.* 39 (6): 1909-1924. doi:10.2134/jeq2009.0462

Ju, B., and Fan, T. 2009. "Experimental Study and Mathematical Model of Nanoparticle Transport in Porous Media." *Powder Technol.* 192 (2): 195-202. doi:10.1016/j.powtec.2008.12.017

Kanj, M. Y., Rashid, H., and Giannelis, E. P. (2011). "Industry First Field Trial of Reservoir Nanoagents," in Paper presented at the SPE Middle East Oil and Gas Show and Conference, Manama, Bahrain, September 2011 (SPE). doi:10.2118/142592-ms

Kmetz, A. A., Becker, M. D., Lyon, B. A., Foster, E., Xue, Z., Johnston, K. P., et al. (2016). Improved Mobility of Magnetite Nanoparticles at High Salinity with Polymers and Surfactants. *Energy fuels.* 30 (3), 1915–1926. doi:10.1021/acs.energyfuels.5b01785

Kotsmar, C., Yoon, K. Y., Yu, H., Ryoo, S. Y., Barth, J., Shao, S., et al. (2010). Stable Citrate-Coated Iron Oxide Superparamagnetic Nanoclusters at High Salinity. *Ind. Eng. Chem. Res.* 49 (24), 12435–12443. doi:10.1021/ie1010965

Kunz, W. (2010). Specific Ion Effects in Colloidal and Biological Systems. *Curr. Opin. Colloid & Interface Sci.* 15 (1-2), 34–39. doi:10.1016/j.cocis.2009.11.008

Li, X., and Shantz, D. F. (2010). Specific Ion Effects on Nanoparticle Stability and Organocation–Particle Interactions in Tetraalkylammonium–Silica Mixtures. *Langmuir* 26 (23), 18459–18467. doi:10.1021/la1035129

Li, Y., Wang, Y., Pennell, K. D., and Abriola, L. M. (2008). Investigation of the Transport and Deposition of Fullerene (C60) Nanoparticles in Quartz Sands under Varying Flow Conditions. *Environ. Sci. Technol.* 42 (19), 7174–7180. doi:10.1021/es801305y

López-León, T., Jódar-Reyes, A. B., Ortega-Vinuesa, J. L., and Bastos-González, D. (2005). Hofmeister Effects on the Colloidal Stability of an IgG-Coated Polystyrene Latex. *J. colloid interface Sci.* 284 (1), 139–148.

Lynn, J. D., and Nasr-El-Din, H. A. (1998). Evaluation of Formation Damage Due to Frac Stimulation of a Saudi Arabian Clastic Reservoir. *J. Petroleum Sci. Eng.* 21 (3), 179–201. doi:10.1016/S0920-4105(98)00074-6

Matteucci, M. E., Paguio, J. C., Miller, M. A., Williams Iii, R. O., and Johnston, K. P. (2008). Flocculated Amorphous Nanoparticles for Highly Supersaturated Solutions. *Pharm. Res.* 25 (11), 2477–2487. doi:10.1007/s11095-008-9659-3

McElfresh, P., Wood, M., and Ector, D. (2012). "Stabilizing Nano Particle Dispersions in High Salinity, High Temperature Downhole Environments," in Paper presented at the SPE International Oilfield Nanotechnology Conference and Exhibition, Noordwijk, The Netherlands, June 2012 (SPE). doi:10.2118/154758-ms

Molina-Bolıvar, J. A., Galisteo-Gonzalez, F., and Hidalgo-Alvarez, R. (1998). Anomalous Colloidal Stability of Latex-Protein Systems. *J. colloid interface Sci.* 206 (2), 518–526.

Molina-Bolívar, J. A., Galisteo-González, F., and Hidalgo-Alvarez, R. (1997). Colloidal Stability of Protein-Polymer Systems: A Possible Explanation by Hydration Forces. *Phys. Rev. E* 55 (4), 4522.

Molina-Bolivar, J. A., Galisteo-González, F., and Hidalgo-Alvarez, R. (1999). The Role Played by Hydration Forces in the Stability of Protein-Coated Particles: Non-classical DLVO Behaviour. *Colloids Surfaces B Biointerfaces* 14 (1-4), 3–17.

Mondal, K., Jegadeesan, G., and Lalvani, S. B. (2004). Removal of Selenate by Fe and NiFe Nanosized Particles. *Ind. Eng. Chem. Res.* 43 (16), 4922–4934. doi:10.1021/ie030715l10.1021/ie030715l

Morr, S., Cuartas, E., Alwattar, B., and Lane, J. M. (2006). How Much Calcium Is in Your Drinking Water? A Survey of Calcium Concentrations in Bottled and Tap Water and Their Significance for Medical Treatment and Drug Administration. *HSS J.* 2 (2), 130–135. doi:10.1007/s11420-006-9000-9

Nabhani, N., Emami, M., Moghadam, A. B. T., Iskandar, F., and Abdullah, M. (2011). Application of Nanotechnology and Nanomaterials in Oil and Gas Industry. *AIP Conf. Proc.* 1415 (1), 128–131. doi:10.1063/1.3667238

Nelson, N., Port, J., and Pandey, M. (2020). Use of Superparamagnetic Iron Oxide Nanoparticles (SPIONs) via Multiple Imaging Modalities and Modifications to Reduce Cytotoxicity: An Educational Review. *Jnt* 1 (1), 105–135. doi:10.3390/jnt1010008

Pfeiffer, C., Rehbock, C., Hühn, D., Carrillo-Carrion, C., de Aberasturi, D. J., Merk, V., et al. (2014). Interaction of Colloidal Nanoparticles with Their Local Environment: the (Ionic) Nanoenvironment Around Nanoparticles Is Different from Bulk and Determines the Physico-Chemical Properties of the Nanoparticles. *J. R. Soc. Interface.* 11 (96), 20130931. doi:10.1098/rsif.2013.0931

Ponnapati, R., Karazincir, O., Dao, E., Ng, R., Mohanty, K. K., and Krishnamoorti, R. (2011). Polymer-Functionalized Nanoparticles for Improving Waterflood Sweep Efficiency: Characterization and Transport Properties. *Ind. Eng. Chem. Res.* 50 (23), 13030–13036. doi:10.1021/ie201925710.1021/ie2019257

Principles of Colloid and Surface Chemistry (1997). Editors P. C. Hiemenz and R. Rajagopalan. 3rd ed. (New York: Marcel Dekker).

Saleh, N., Kim, H.-J., Phenrat, T., Matyjaszewski, K., Tilton, R. D., and Lowry, G. V. (2008). Ionic Strength and Composition Affect the Mobility of Surface-Modified Fe0 Nanoparticles in Water-Saturated Sand Columns. *Environ. Sci. Technol.* 42 (9), 3349–3355. doi:10.1021/es071936b

Santander-Ortega, M. J., Peula-García, J. M., Goycoolea, F. M., and Ortega-Vinuesa, J. L. (2011). Chitosan Nanocapsules: Effect of Chitosan Molecular Weight and Acetylation Degree on Electrokinetic Behaviour and Colloidal Stability. *Colloids Surfaces B Biointerfaces* 82 (2), 571–580. doi:10.1016/j.colsurfb.2010.10.019

Santander-Ortega, M. J., Stauner, T., Loretz, B., Ortega-Vinuesa, J. L., Bastos-González, D., Wenz, G., et al. (2010). Nanoparticles Made from Novel Starch Derivatives for Transdermal Drug Delivery. *J. Control. release* 141 (1), 85–92. doi:10.1016/j.jconrel.2009.08.012

ShamsiJazeyi, H., Miller, C. A., Wong, M. S., Tour, J. M., and Verduzco, R. (2014). Polymer-coated Nanoparticles for Enhanced Oil Recovery. *J. Appl. Polym. Sci.* 131 (15), a–n. doi:10.1002/app.40576

Tassa, C., Shaw, S. Y., and Weissleder, R. (2011). Dextran-coated Iron Oxide Nanoparticles: a Versatile Platform for Targeted Molecular Imaging, Molecular Diagnostics, and Therapy. *Acc. Chem. Res.* 44 (10), 842–852. doi:10.1021/ar200084x

Unterweger, H., Dézsi, L., Matuszak, J., Janko, C., Poettler, M., Jordan, J., et al. (2018). Dextran-coated Superparamagnetic Iron Oxide Nanoparticles for Magnetic Resonance Imaging: Evaluation of Size-dependent Imaging Properties, Storage Stability and Safety. *Ijn* 13, 1899–1915. doi:10.2147/ijn.S156528

Vereda, F., Martín-Molina, A., Hidalgo-Alvarez, R., and Quesada-Pérez, M. (2015). Specific Ion Effects on the Electrokinetic Properties of Iron Oxide Nanoparticles: Experiments and Simulations. *Phys. Chem. Chem. Phys.* 17 (26), 17069–17078. doi:10.1039/c5cp01011j

Worthen, A. J., Tran, V., Cornell, K. A., Truskett, T. M., and Johnston, K. P. (2016). Steric Stabilization of Nanoparticles with Grafted Low Molecular Weight Ligands in Highly Concentrated Brines Including Divalent Ions. *Soft Matter* 12 (7), 2025–2039. doi:10.1039/c5sm02787j

Xue, Z., Foster, E., Wang, Y., Nayak, S., Cheng, V., Ngo, V. W., et al. (2014). Effect of Grafted Copolymer Composition on Iron Oxide Nanoparticle Stability and Transport in Porous Media at High Salinity. *Energy fuels.* 28 (6), 3655–3665. doi:10.1021/ef500340h10.1021/ef500340h

Yu, J., Cheng, A., Mo, D., Liu, N., and Lee, R. (2012). "Study of Adsorption and Transportation Behavior of Nanoparticles in Three Different Porous Media," in Paper presented at the SPE Improved Oil Recovery Symposium, Tulsa, Oklahoma, USA, April 2012 (SPE). doi:10.2118/153337-ms

Yu, Jie, Berlin, J. M., Lu, W., Zhang, L., Kan, A. T., Zhang, P., et al. (2010). "Transport Study of Nanoparticles for Oilfield Application," in Paper presented at the SPE International Conference on Oilfield Scale, Aberdeen, UK, May 2010 (SPE). doi:10.2118/131158-ms

Zhang, T., Murphy, M. J., Yu, H., Bagaria, H. G., Yoon, K. Y., Neilson, B. M., et al. (2015). Investigation of Nanoparticle Adsorption during Transport in Porous Media. *SPE J.* 20 (04), 667–677. doi:10.2118/166346-pa

Zhang, Y., and Cremer, P. (2006). Interactions between Macromolecules and Ions: the Hofmeister Series. *Curr. Opin. Chem. Biol.* 10 (6), 658–663. doi:10.1016/j.cbpa.2006.09.020

Zhao, X., Liu, W., Cai, Z., Han, B., Qian, T., and Zhao, D. 2016. "An Overview of Preparation and Applications of Stabilized Zero-Valent Iron Nanoparticles for Soil and Groundwater Remediation." *Water Res.* 100: 245-266. doi:10.1016/j.watres.2016.05.019

**Conflicts of Interest:** Authors RS, HO, JC, AK and HC were employed by the company Aramco Americas.

The authors declare that this study received involvement from Saudi Aramco and Aramco Services Company. The company was involved in the decision to submit it for publication.

**Publisher's Note:** All claims expressed in this article are solely those of the authors and do not necessarily represent those of their affiliated organizations, or those of the publisher, the editors and the reviewers. Any product that may be evaluated in this article, or claim that may be made by its manufacturer, is not guaranteed or endorsed by the publisher.